Journal of the European Ceramic Society **17** (1997) 1749–1755

PII: S0955-2219(97)00031-9
0955-2219/97/$17.00

Ferroelectric Properties of PZT Thin Films Prepared by Sputtering with Stoichiometric Single Oxide Target: Comparison Between Conventional and Rapid Thermal Annealing

G Velu, D. Remiens & B. Thierry

Laboratoire des Matériaux Avancés Céramiques, CRITT 'Céramiques Fines', Université de Valenciennes et du Hainaut-Cambrésis, Z.I. Champ de l'Abbesse – 59600 Maubeuge – France

(Received 4 November 1996; accepted 10 February 1997)

Abstract

The influence of growth conditions and post-annealing treatments on radio frequency (r.f.) *magnetron sputtered lead zirconate titanate (PZT) thin films have been investigated. By adjusting the plasma discharge parameters, it is possible to control, with stoichiometric single oxide target, the film composition precisely. No excess lead was used either during sputtering (in the target) or during post-deposition annealing. The structural, microstructural and electrical properties have been systematically examined as a function of the annealing treatments. Perovskite structure was obtained by conventional annealing as well as by rapid thermal annealing. The films were dense and crack-free; the film orientation, the microstructure and the surface morphology are directly related to the thermal processes. The ferroelectric properties in terms of coercive field and remanent polarization are also very sensitive to the annealing treatments.* © *1997 Elsevier Science Limited.*

Resumé

L'influence des conditions de dépôt et de recuit post-dépôt sur la croissance, par pulvérisation cathodique (r.f) *magnétron, de films minces de titanozirconate de plomb est étudiée. En ajustant les paramètres de la décharge, il est possible de contrôler précisément, à partir d'une cible d'oxydes multi-éléments, la composition des films. L'ajout d'un excés de plomb, aussi bien dans la phase de dépôt (au niveau de la cible) que dans la phase de recuit post-dépôt s'est avéré inutile. Les propriétés structurales, microstructurales et électriques ont été systématiquement examinées en fonction des traitements thermiques. La structure pérovskite a été obtenue aussi bien par recuit conventionnel que par recuit rapide. Les films sont denses et sans fissure; l'orientation des films et leurs microstructures sont directement reliés à la nature du traitement thermique. Les propriétés ferroélectriques sont également étroitement correllées au traitement thermique post-dépôt.*

1 Introduction

Lead zirconate titanate [$Pb(Zr,Ti)O_3$ or PZT] is a well-known ferroelectric and piezoelectric material. PZT films have attracted great attention in recent years as promising material for use in nonvolatile memories[1,2] and in microelectromechanical systems.[3,4] The growth of PZT thin films has been realized by various methods.[5,6,7] Single target sputtering is likely to be a dominant growth technique for PZT thin films because the simplest process meeting the device fabrication requirements is the most desirable. However this method presents some disadvantages,[8] such as compositional changes in the film from the target.

One of the primary factors in the synthesis and crystallisation of PZT films is proper control of the lead content of the films. This is due to the fact that lead tends to re-evaporate easily at elevated temperatures and currently targets with excess amounts of PbO are used in order to compensate for the loss that may occur during heating deposition or post-deposition annealing.[9] While the majority of previous depositions were with targets containing excess lead oxide, only a few reports[10] are available regarding the sputter deposition of

stoichiometric single-oxide targets without excess lead. Recent results suggest that a mechanism of perovskite formation may depend on the target composition.[11] In the present work, the compositional modifications of PZT films with sputtering conditions are investigated and the above problem in single target sputtering process is solved. No excess lead was used during sputtering.

The influence of post-deposition annealing treatments and conditions on structural and microstructural properties have also been investigated. Conventional heating (tubular furnace) and Rapid Thermal Annealing (RTA) have been compared. The main advantage of the RTA process is to avoid (or to limit) the eventual degradation of the film–substrate interface[12] (interdiffusion of lead). The RTA was found to have significant influence on the crystallisation behavior. Either (110) or (100) highly oriented PZT films can be obtained depending on the annealing treatments. The ferroelectric properties have been measured; they are very sensitive to the annealing treatments.

2 Film preparation

PZT thin films, with composition near the morphotropic phase, were prepared on $Si/SiO_2/Ti/Pt$ substrates by *r.f.* magnetron sputtering; the system deposition has been described previously.[13] On a 5000 Å thick thermal oxide, a Ti/Pt bottom electrode was deposited by sputtering without substrate heating. Their thicknesses are respectively 200 Å and 2000 Å in order to suppress the formation of hillocks.[14,15] The single oxide target was cold pressed powder whose diameter and thickness were 75 mm and 3 mm respectively. The powder used was a stoichiometric mixture of the three oxides in the composition 54/46 (Zr/Ti). The chamber is evacuated with a turbomolecular pump to a pressure below $5 \cdot 10^{-7}$ Pa before deposition. The films were performed at room temperature; in order to stabilize the target composition (formation of the 'altered layer')[16] a pre-sputtering is necessary. The pre-sputtering conditions are similar to those used during the film deposition.

3 Experimental results and discussion

3.1 Composition

The chemical composition of the PZT films was determined by energy dispersion spectroscopy (EDS). The compositional changes of PZT films with sputtering conditions are investigated; the major objective is to determine the 'working point', i.e. the sputtering parameters which provide a film composition similar to the target composition, i.e. PZT (54/46). The lead content in the films was found to change with sputtering gas pressure, as show in Fig. 1. Sputtered at a lower gas pressure (in the range 10–25 mT) the lead content in the film is less than that of the target. It approaches the target composition as the pressure is increased; at 30 mT the ratio Pb/Zr + Ti is nearly equal to 1. For higher pressure (> 50 mT) the composition is constant (Pb/Zr + Ti = 1·2). On the other hand, the Zr/Ti ratios of the films were almost equal to that of the target, irrespective of the sputtering gas pressure. This compositional change may be caused by preferential resputtering by accelerated negative ions[17] and by a dispersion effect of the sputtered species in the plasma.[18] The film composition is also affected by *r.f.* power; Fig. 2 shows *r.f.* power dependence of film composition. The lead content in the films increases with the *r.f.* power; the Zr/Ti ratios were constant. We have fixed the *r.f.* power density to 2·36 W cm^{-2}; for higher power, cracks appear at the surface target in the erosion area (magnetron cathode).

The target–substrate distance is an important parameter which also controls the film composition (Fig. 3). It should be noted that the Zr/Ti ratio changes only slightly, while the lead content changes strongly over the interelectrodes distance range which is from 40 mm to 70 mm. This behavior is also directly related to the scattering effect of the species in the plasma;[19] it is more pronounced for heavy ions such as lead ions.[20] In order to have a good thickness homogeneity, we have fixed the target–substrate distance to 60 mm.

The selected sputtering conditions are summarized in Table 1; with these parameters the growth rate is in the order of 50 Å/min. Nearly stoichiometric films were obtained with simple single-oxide

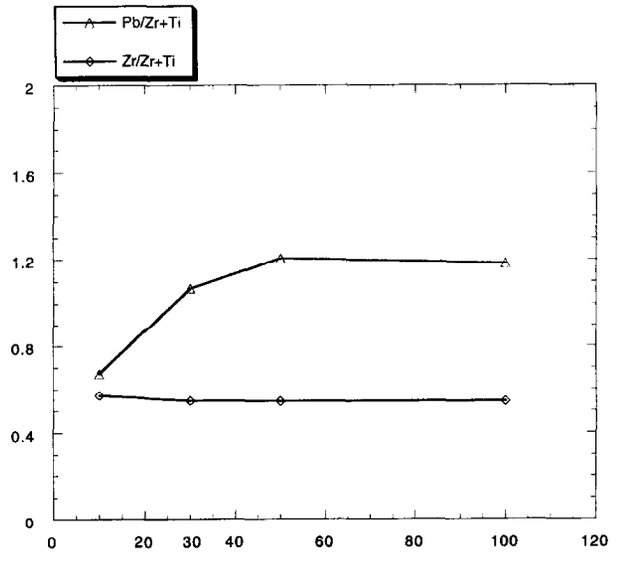

Fig. 1. Sputtering gas pressure dependence of film composition.

targets. More precisely, the films contain a small excess of lead (Pb/Zr+Ti=1·1). We have made this choice since in general it has been observed that the presence of excess Pb in the film favors perovskite phase formation. The lead excess is evaporated during the annealing treatments.

These results show that the PZT film composition and in particular the lead content in the film can be easily and precisely adjusted (and controlled) by way of the plasma discharge parameters. This is an important advantage of the sputtering deposition technique.

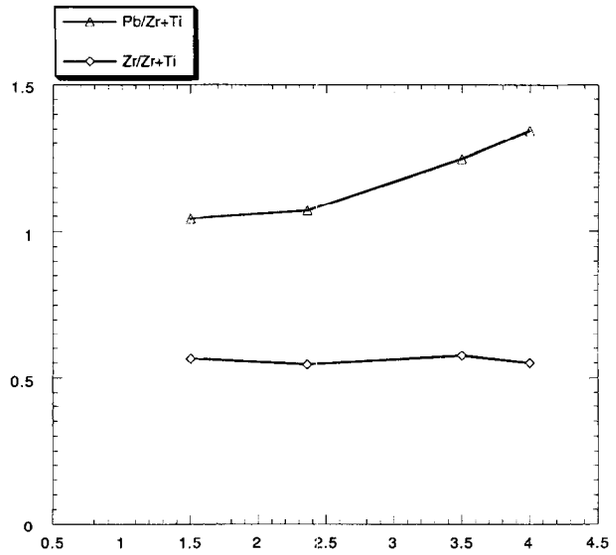

Fig. 2. R.F. power dependence of film composition.

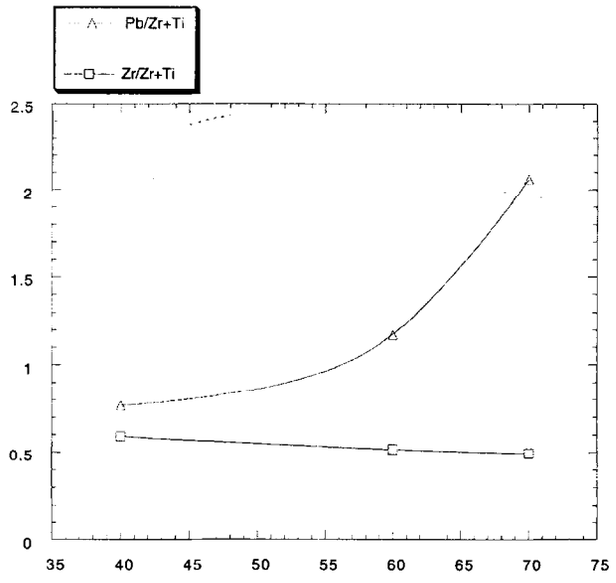

Fig. 3. Interelectrodes distance dependence of film composition.

Table 1. Optimized sputtering conditions for preparation of PZT (54/46) films

R.F. power density	2·36 W cm^{-2}
Target diameter	75 mm
Target composition	PZT (54/46) without lead excess
Interelectrodes distance	60 mm
Gas pressure	30 mT
Sputtering gas	Ar
Substrate temperature	Ambiant

3.2 Crystallographic structure

As we have mentioned previously, deposition of PZT film was performed at room temperature and consequently the films are amorphous. A post-deposition annealing is then required to achieve a well-crystallized perovskite structure. This thermal treatment also allows the removal of the porosities in the film (densification). We have compared this situation with the structural properties obtained on PZT films annealed with conventional treatment (tubular furnace) and rapid thermal process. Rapid thermal processing (RTP) of ferroelectric films is found to have advantages over conventional furnace annealing.[21] Rapid annealing of films at a high temperature for very short periods (a few seconds) may reduce the reaction between the film and the substrate.[22,23] The capability of controlling grain size by RTP is also of interest for non-volatile memory since smaller grain sizes offer a higher dielectric constant.[24] The crystallographic structure of the films was examined by X-ray diffraction (XRD) in a θ–2θ system using Cu-Kα radiation.

By conventional annealing (the ambiant gas is air) the films are amorphous below 500°C and the perovskite phase appears at 500°C when the annealing time is fixed to 2 h (Fig. 4). The crystallisation was initiated directly in the perovskite phase, the pyrochlore phase did not appear.[25,26] The presence of lead excess in the film favors perovskite temperature phase formation. The phase transformation depends on the initial nature of the as-deposited films such as lead stoichiometry of films[27,28] The direct transformation between amorphous through perovskite phase is directly related to the presence of lead excess in our as-deposited films. When the annealing temperature increased, the crystallinity of PZT films increased, indicated by higher and sharper peaks. Figure 5 shows the XRD patterns of films annealing at 625°C (over 30 min); the film presents a (110) preferred orientation. The ramp down is fixed to 1°C min^{-1}; for higher values micro-cracks appear on films. At higher annealing temperatures and annealing times, the peaks' intensity decreases and the lead-deficient pyrochlore phase appears. The optimized conventional annealing parameters are summarized in Table 2.

The PZT films' crystallisation was also studied by rapid thermal annealing (RTA). The rapid thermal processor essentially contains a bank of 12 tungsten halogen lamps placed above a quartz window, which provide the energy required for

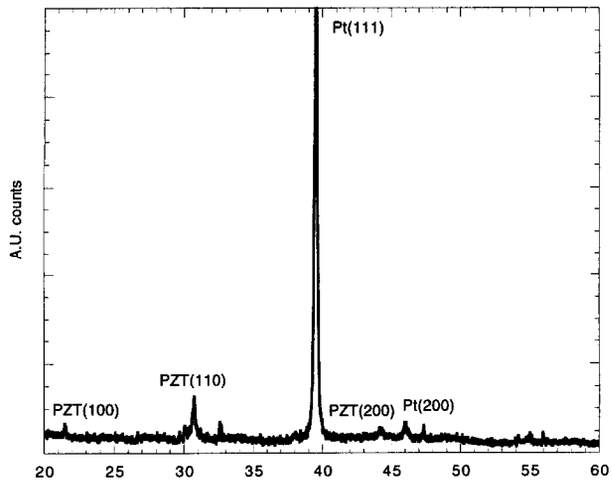

Fig. 4. XRD pattern of PZT film (annealing temperature = 500°C – annealing time = 2 h).

heating the sample. The sample was attached to a susceptor (silicon wafer); the temperature of the system was monitored using a chromel-alumel thermocouple placed on the susceptor. Since PZT is transparent in the infrared region, the film annealing was induced by the heat transfer from the silicon which absorbs most of the incident radiation with wavelength less than 1 μm.

We have optimized the RTA process; more precisely we have determined the annealing profiles to obtain crystallized PZT film (1 μm thick) crack-free and dense.

The perovskite structure, without any second phase, appears at 550°C for 120 s as shown in Fig. 6. At 625°C, which corresponds to the annealing temperature of the conventionnal treatment, the film is very well crystallized (Fig. 7). In this example, the annealing time is limited to 60 s; the heating and cooling rates are 7°C s^{-1} and 100°C s^{-1} respectively. For higher values microcracks appear in the films probably due to the existence of stresses in the film and to the significant mismatch in the thermal expansion coefficients between the film and the substrate. The film is highly (100) textured. By increasing the annealing temperature, it is possible to decrease the annealing time. For example, at 700°C pure perovskite phase was obtained for an annealing time as low as 5 s (Fig. 8); the films are also (100) oriented.

The pure perovskite phase is obtained for a very short annealing duration; this is the most significant of the RTA process which has important effects on the film–substrate interface quality.[12,21] The influence of the atmosphere during annealing (O_2, N_2, ...) is now in progress.

The microstructure of the PZT films, obtained by the two processes, has been systematically observed by scanning electronic microscopy. In general, the films are dense, smooth and crack-free. The most important difference between the two processes is the smaller grain size for films annealed by the RTA process. In RTA, the films are heat-treated for very small durations and therefore the grain growth is limited.

3.3 Ferroelectric properties

The ferroelectric nature of the films was examined by observing the hysteresis loop, taken at room temperature, by means of a RT6000 standard test system. The test capacitors were fabricated with a $Si/SiO_2/Ti/Pt/PZT$ (1 μm thick)/Pt structure. Pt top electrodes were fabricated by photolithography and sputtering (lift-off process). Depending on the annealing processes, some differences have been observed in the ferroelectric performance.

Figure 9 shows a typical polarization versus applied voltage measurement result for a sample conventionally annealed at 625°C over 30 min. It shows a maximum polarisation of 38 μC cm^{-2}, a remanent polarisation of 16 μC cm^{-2} and a coercive field of 30 KV cm^{-1}. This polarisation value is less than that for the bulk ceramics but is comparable to

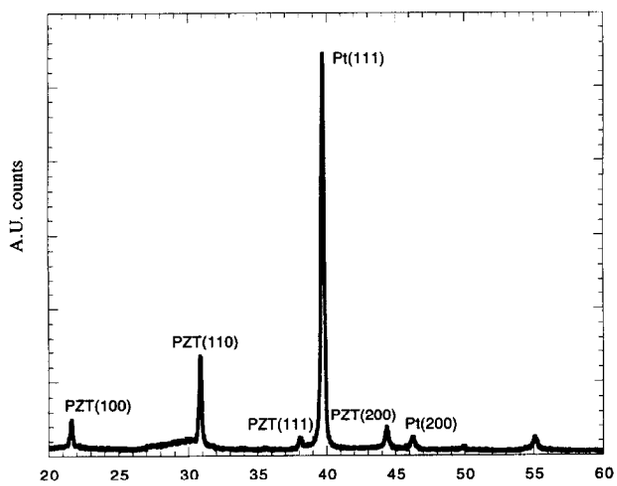

Fig. 5. XRD pattern of PZT film (annealing temperature = 625°C – annealing time = 30 min).

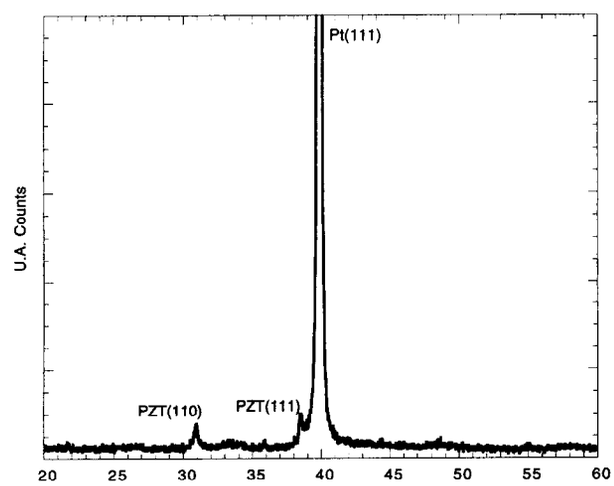

Fig. 6. XRD pattern of PZT film (RTA process — annealing temperature = 550°C — annealing time = 120 s).

those reported for thin film PZT. The coercive field was larger than those of PZT ceramics; this is essentially due to the small grain size and the large stress induced by the thermal expansion mismatch between the film and the substrate. The hysteresis loop showed a small shift along the axis of the electric field. Asymmetric hysteresis loops have been observed by many workers in both bulk ceramics and thin films and originate from internal fields due to space–charge accumulation at the grain boundaries and at the film–electrode interface.[29] Figure 10 shows an hysteresis loop relative to a rapid thermal annealed sample (625°C — 30 s).

Table 2. Selected conventional annealing parameters for PZT films (1 μm thick)

Annealing temperature	625°C
Annealing time	30 min
Heating rate	3°C min^{-1}
Cooling rate	1°C min^{-1}
Gas ambiant	Air

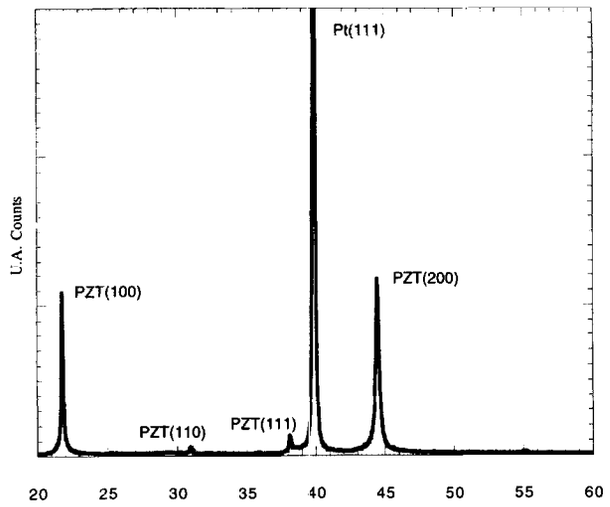

Fig. 7. XRD pattern of PZT film (RTA process — annealing temperature = 625°C — annealing time = 60 s).

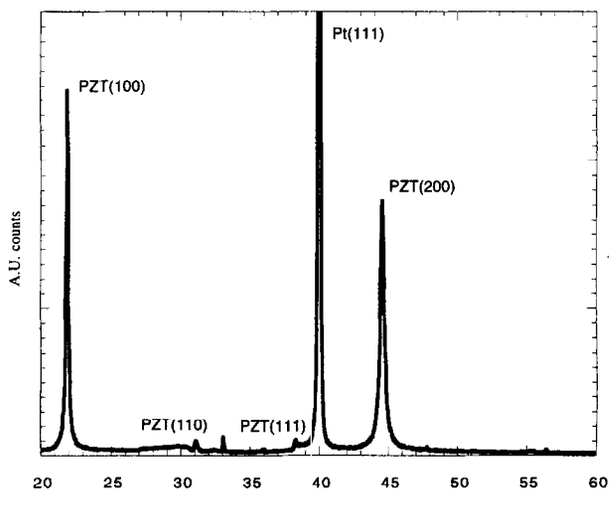

Fig. 8. XRD pattern of PZT film (RTA process — annealing temperature = 700°C — annealing time = 5 s).

The calculated maximum and remanent polarisations are 38 μC cm^{-2} and 20 μC cm^{-2} respectively; the coercive field is 53 KV cm^{-1}. The saturation polarisation is not reached for PZT-RTA films at 20 V. By comparison with conventional annealing, more important bias voltage is necessary to attain the saturation, typically 35 V. At this voltage important leakage current appears. The high value of the coercive field (53 KV cm^{-1}) shows that it is more difficult to switch the domains for PZT-RTA films rather than PZT conventionally annealed films (30 KV cm^{-1}).

This could be a consequence of a smaller grain size in comparison with conventional treatment (for the faster heating rate, a smaller grain size is obtained) and important stresses stored in the RTA films (high-heating rate). Identical results have been obtained on films and doped bulk ceramics.[30] The different alignments of the films (100) and (110) for rapid thermal and conventional annealing respectively also have an important effect on the ferroelectric properties of the films.[31]

Loss of polarization with repetitive voltage switching, which is called fatigue, has been an important issue related to the reliability of ferroelectric thin film devices such as nonvolatile random access memories. We have compared the fatigue characteristics of PZT films annealing by the two processes. The capacitors under test were subjected to a sinusoidal voltage of 20 V at frequency of 1 kHz with intermittent interruptions for hysteresis measurement. Since the bias voltage is limited to 20 V (experimental set-up limitation) the PZT-RTA films were not allowed to reach their saturation polarisation. So, the experimental results obtained in these films were not representative of their fatigue characteristics, Fig. 11 shows a typical fatigue characteristic of the films. The P_r values reduced by 17% after 10^7 cycles and 21%

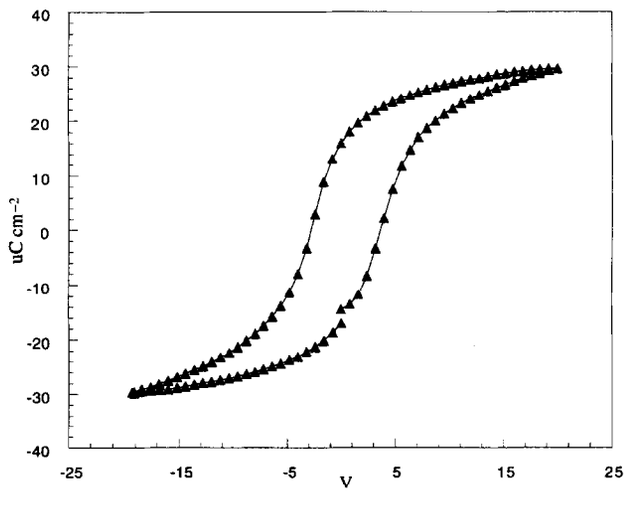

Fig. 9. Typical hysteresis loop of conventionally annealed (T = 625°C — t = 30 min) PZT film.

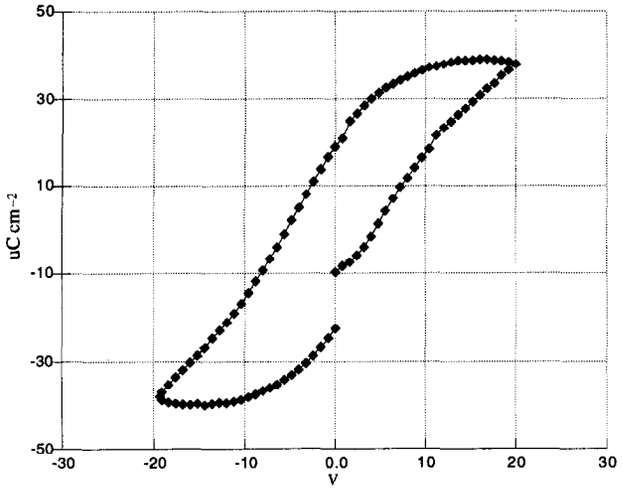

Fig. 10. Typical hysteresis loop of rapid thermal annealed (T = 625°C — t = 30 s) PZT film.

after 10^9 cycles for conventionally annealed films and the coercive field increased by 30% after 10^9 cycles. This result is in perfect agreement with most previous works performed on PZT films with Pt electrodes, which reported a large loss of polarization after 10^6–10^9 cycles.[32] Pt electrodes (top and bottom) are not well adapted for memories applications, new electrodes such as RuO_2, $LaSrCoO_3$, present better fatigue characteristics.[33,34] We have made some annealing treatments on the top sputter-deposited Pt electrode. Recent results show that the ferroelectric properties can be improved during annealing of the top electrode.[35] Two annealing temperatures have been tested: 450 and 500°C; the annealing time was fixed to 1 h. The asymmetry of the hysteresis loop tends to disappear when the top electrodes are annealed but any modification of the fatigue characteristics have been observed. Studies, such as optimization of annealing Pt electrodes (top and bottom), modification of the structure (in particular the presence of a buffer layer between the film and the electrode) are now in progress.

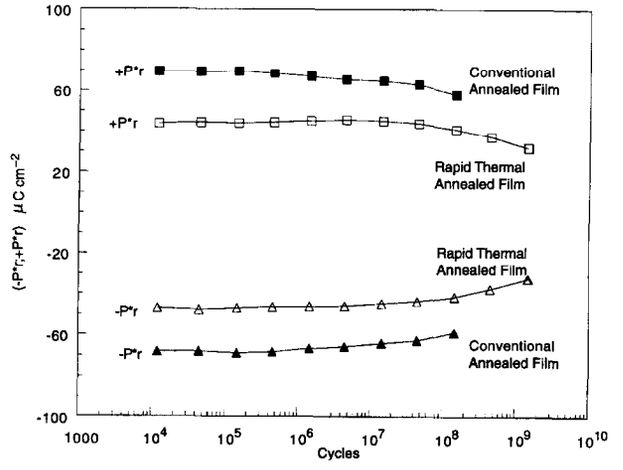

Fig. 11. Fatigue characteristics of conventionally and rapid thermal annealed PZT films.

4 Conclusion

Precise composition control was achieved in a stoichiometric single-oxide target sputtering process for ferroelectric PZT thin films. Since lead content in the films changes in proportion to gas pressure and *r.f.* power, we can adjust the film composition accurately by way of the sputtering parameters. The crystallisation of the films has been studied in relation to conventional annealing as well as rapid thermal annealing. The structure and the microstructure of the films are very sensitive to the post-thermal process. Highly (100) oriented films are obtained by RTA and (110) oriented films are obtained by conventional annealing.

The ferroelectric properties are also directly related to the annealing processes.The coercive field of the PZT-RTA film is much higher than that of conventionally annealed films. The grain size, the stresses stored in the films and the films' orientation are essentially responsible for this increase. The fatigue characteristics show a degradation of the ferroelectric properties which can be attributed to the presence of the Pt electrodes (top and bottom). New structures such as $Si/SiO_2/Ti/Pt/PbTiO_3/PbZrTiO_3/Pt$ are now in progress; recent publications show that the presence of a $PbTiO_3$ buffer layer improves the fatigue characteristics.

Acknowledgement

The authors would like to thank the Nord-Pas de Calais Country for his partial financial support of this study.

References

1. Araujo, C. A., McMillan, L. D., Melnick, B. M., Cuchiaro, J. D. and Scott, J. F., *Ferroelectrics*, 1990, **104**, 241.
2. Scott, J. F. and Araujo, C. A., *Science*, 1989, **246**, 1400.
3. Polla, D. L., Ye, C. and Tamagawa, T., *Appl. Phys. Lett.*, 1991, **59**, 3539.
4. Muralt, P., *10th International Symposium on Applications of Ferroelectrics (ISAF'96)*, paper 3A.1, New-Breswick, 1996.
5. Budd, K. D., Dey, S. K. and Payne, D. A., *Br. Ceram. Proc.*, 1985, **36**, 107.
6. Auciello, O., Mantese, L., Duarte, J., Chen, X, Rou, S. H., Kingon, A. I., Schreiner, A. F. and Krauss, A. R., *Journal of Appl. Phys.*, 1993, **73**, 5197.
7. De Kaiser, M., Dormans, G. J. M., Van Veldhoven, P. J. and Lansen, P. K., *Integrated Ferro-electrics*, 1993, **3**, 131.
8. Nakagawa, T., Yamaguchi, J., Okuyama, M. and Hamakawa, Y., *Jpn. Journal of Appl. Phys.*, 1982, **21**, 1655.
9. Takayama, R. and Tomita, Y., *Journal of Appl. Phys.*, 1989, **65**, 1666.
10. Basit, N. A. and Kim Hong Koo, , *Journal of Vac. Sci. Technol.*, 1995, **A13**(4), 221.
11. Li, X., Liu, J. and Liang, J., *Appl. Phys. Lett.*, 1993, **63**, 2345.

12. Vasant Kumar, C. V. R., Sayer, M., Pascual, R., Amm, D. T., Wu, Z. and Swanston, D. M., *Appl. Phys. Lett.*, 1991, **58**, 1161.
13. Rèmiens, D., Jaber, B., Tirlet, J. F., Joire, H., Thierry, B. and Moriamez, Cl., *Journal of Eur. Ceram. Soc.*, 1994, **13**, 493.
14. Sreenivas, K., Reaney, I. Maeder, T. and Setter, N., *Journal of Appl. Phys.*, 1994, **75**, 232.
15. Rèmiens, D., Jaber, B., Tronc, P. and Thierry, B., *Journal of Eur. Ceram. Soc.*, 1996, **16**, 467.
16. Wehner, G. J., *Journal of Vac. Sci. Technol.*, 1983, **A1**, 487.
17. Sreenivas, K., Sayer, M. and Garrett, P., *Thin Solid Films*, 1989, **172**, 251.
18. Vasant Kumar, C. V. R. and Mansingh, A., *Journal of Appl. Phys.*, 1989, **65**, 1270.
19. Chapman, B., *Glow dischange processes*, John Wiley & Sons, New York, 1980.
20. Mansingh, A. and Krupanidhi, S. B., *Journal of Appl. Phys.*, 1980, **51**, 5408.
21. Vasant Kumar, C. V. R., Pascual, R. and Sayer, M., *Journal of Appl. Phys.*, 1992, **71**, 864.
22. Brooks, K., Klissurska, R., Moeckli, P. and Setter, N., *Microelectronic Eng.*, 1995, **29**, 293
23. Brooks, K., Reaney, Ian M., Klissurska, R., Huang, Y., Bursill, L. and Setter, N., *Journal of Mat. Res.*, 1994, **9**, 2540.
24. Haertling, G. H., *Bull. Am. Ceram. Soc.*, 1964, **43**, 875.
25. Yi, G., Wu, Z. and Sayer, M., *Journal of Appl. Phys.*, 1988, **64**, 2717.
26. Okada, M., Tominaga, T., Araki, T., Katayama, S. and Sakashita, Y., *Jpn. Journal of Appl. Phys.*, 1990, **29**, 718.
27. Klee, M., Eusemann, R., Waser, R. and Brand, W., *Journal of Appl. Phys.*, 1992, **72**, 1566.
28. Torii, K., Kaga, T., Kushida, K., Takeuchi, H. and Takeda, E., *Jpn. Journal of Appl. Phys.*, 1991, **30**, 3562.
29. Fukami, T. and Fujü, S., *Jpn. Journal of Appl. Phys.*, 1985, **24**, 632.
30. Okazaki, K. and Nagata, K., *Journal of Am. Ceram. Soc.*, 1973, **56**, 82.
31. Kim, C. J., Yoon, D. S., Lee, J. S. and Choi, C. G., *Journal of Appl. Phys.*, 1994, **76**, 7478.
32. Colla, E. L., Kholkin, A. L., Taylor, D., Tagantsev, A. K., Brooks, K. G. and Setter, N., *Micro-electronic Engineering*, 1995, **29**, 145.
33. Spierings, G. A. C. M., Breed, J. M., Ulenaers, M. J. E., Van Veldhoven, P. J. and Larsen, P. K., *Microelectronic Engineering*, 1995, **29**, 235.
34. Ramesh, R., Gilchrist, H., Sands, T., Keramidas, V. G., Haakenasen, R. and Fork, D. K., *Appl. Phys. Lett.*, 1993, **63**, 3592.
35. Lee, E. G., Wouters, Dirk J., Willems, G. and Maes, Herman E., *Appl. Phys. Lett.*, 1996, **69**, 1223.